

SUPERSYMMETRY (AT LARGE $\tan \beta$) AND FLAVOUR PHYSICS

PIOTR H. CHANKOWSKI^a AND JANUSZ ROSIEK^{a,b}

^aInstitute of Theoretical Physics, Warsaw University
Hoża 69, 00-681 Warsaw, Poland

^bPhysik Department, Technische Universität München
D-85748 Garching, Germany

(Received July 3, 2002)

Dedicated to Stefan Pokorski on his 60th birthday

Recent development in exploring flavour dynamics in the supersymmetric extension of the Standard Model is reviewed. Emphasis is put on possible interesting effects in b -physics arising for large values of $\tan \beta$ both in the case of minimal flavour violation and in the case of flavour violation originating in the sfermion sector. The importance of the flavour changing neutral Higgs boson couplings generated by the scalar penguin diagrams and their role in the interplay of neutral B -meson mixing and $B_{d,s}^0 \rightarrow \mu^+ \mu^-$ decays is discussed. It is pointed out that observation of the $B_d^0 \rightarrow \mu^+ \mu^-$ decay with BR at the level $\gtrsim 3 \times 10^{-8}$ would be a strong indication of non-minimal flavour violation in the quark sector. Possible impact of flavour violation in the slepton sector on neutrino physics is also discussed.

PACS numbers: 12.15.Mm, 12.60.Jv, 13.20.He, 14.60.Pq

1. Introduction

Physics of flavour and of CP violation continues to be an interesting subject to study in various extensions of the Standard Model (SM). On one hand, before the advent of LHC and linear colliders, which will enable us to probe energies much above the electroweak scale directly, rare processes intensively studied in numerous experiments are the first place where the effects of new physics — *i.e.* virtual effects of new particles — can most likely be detected. On the other hand, studies of baryogenesis [1] strongly suggest that the SM with its unique source of CP violation and known particle content is unable to explain the baryon to photon density number ratio, $n_B/n_\gamma \sim 10^{-9}$, observed in the Universe, given the present lower limit on

the Higgs boson mass. This supports expectations that some deviations from the SM predictions will eventually be encountered in the ongoing or planned precision studies of rare and CP violating processes. Finally, the first direct indication of inadequacy of the SM has also to do with flavour physics — namely with neutrino oscillations. Explanation of the observed neutrino oscillations requires the introduction of flavour mixing (and perhaps also of CP violation) in the lepton sector. While the SM can easily be extended to describe neutrino oscillations, there are strong theoretical arguments that the observed phenomena have their origin in physics at energy scales much higher than the electroweak scale.

Physics of flavour in the framework of supersymmetric extension of the Standard Model was also always in the centre of Stefan Pokorski's interest. It is therefore a pleasure to devote this article to him. The subject is of course too vast to be reviewed here in all details. Instead we concentrate on its most interesting in our opinion aspects. These include recent investigations of the supersymmetric effects in b -physics arising for large $\tan\beta$ and in the neutrino sector. In this context it is appropriate to recall here that systematic investigations of supersymmetry at large $\tan\beta$ begun with the Stefan Pokorski's seminal paper [2].

2. Flavour violation: minimal and generalised minimal

Extensions of the SM can be divided into two broad classes: models in which the Cabibbo–Kobayashi–Maskawa matrix (CKM) in the quark sector and Maki–Nakagawa–Sakata matrix (MNS) in the lepton sector are the only sources of flavour and CP violation and models in which there are entirely new sources of flavour and/or CP violation. Both options can be realized independently in the quark and lepton sectors of the simplest supersymmetric extension of the SM — the MSSM — and it is the experimental task of utmost importance to establish which one is realized in Nature.

If the CKM matrix is the only source of flavour and CP violation in the quark sector, the natural question is what is the impact of new physics on the determination of its elements. In particular one wants to know the value of the V_{td} element which is needed *e.g.* to predict the rate of the decay $B_d^0 \rightarrow \mu^+ \mu^-$ and other interesting rare processes. It is also important to see if the consistency of the determination of the CKM matrix elements from different processes imposes any constraints on the MSSM parameters.

The CKM matrix V is most conveniently parameterised as follows [3]:

$$V = \begin{pmatrix} 1 - \lambda^2/2 & \lambda & A\lambda^3(\rho - i\eta) \\ -\lambda & 1 - \lambda^2/2 & A\lambda^2 \\ A\lambda^3(1 - \rho - i\eta) & -A\lambda^2 & 1 \end{pmatrix} + \mathcal{O}(\lambda^4).$$

The Wolfenstein parameters $\lambda \approx 0.222 \pm 0.0018$ and $A \approx 0.83 \pm 0.06$ are rather accurately determined from transitions dominated by tree level contributions, and are hence insensitive to new physics. At present, processes of this kind put also some constraints on the remaining two (conveniently rescaled [4]) parameters $\bar{\rho} \equiv \rho(1 - \lambda^2/2)$ and $\bar{\eta} \equiv \eta(1 - \lambda^2/2)$. The value of the combination $R_b \equiv \sqrt{\bar{\rho}^2 + \bar{\eta}^2}$ is constrained to $0.27 \lesssim R_b \lesssim 0.46$ by the result $|V_{ub}|/|V_{cb}| = 0.08 \pm 0.02$ (at 95 % C.L.) extracted from the charmless B decays. The CP violating time dependent asymmetry in the $B \rightarrow \psi K_S$ decay constrains the phase β_{ut} of the V_{td} element: $V_{td} = |V_{td}|e^{-i\beta_{\text{ut}}}$. In minimal models this asymmetry is simply given by $\sin 2\beta_{\text{ut}}$. The average of the measurements done at BaBar and Belle gives $\sin 2\beta_{\text{ut}} = 2\bar{\eta}(1 - \bar{\rho})/\sqrt{(1 - \bar{\rho})^2 + \bar{\eta}^2} = 0.78 \pm 0.08$ [5]. There are also prospects for extracting from such processes also the phase γ_{ut} of the V_{ub} element: $V_{ub} = |V_{ub}|e^{-i\gamma_{\text{ut}}}$. However, large theoretical and experimental uncertainties still prevent precise determination of $\bar{\rho}$ and $\bar{\eta}$ exclusively from tree level dominated processes.

Parameters $\bar{\rho}$ and $\bar{\eta}$ are also extracted from measurements of the $B_{s,d}^0 - \bar{B}_{s,d}^0$ meson mass differences $\Delta M_{s,d}$ and of the parameter ε_K of CP violation in the neutral kaon system. This allows to overconstrain the values of $\bar{\rho}$ and $\bar{\eta}$ and test the assumption of minimal flavour and CP violation in the quark sector. However, since all the three quantities are loop induced, the new physics can contribute to relevant amplitudes. Therefore, the values of $\bar{\rho}$ and $\bar{\eta}$ determined from $\Delta M_{s,d}$ and ε_K can significantly depend on new physics. One can also expect that consistency of the CKM parameters determination puts some constraints on new physics.

To compute $\Delta M_{s,d}$ and ε_K one integrates out from the theory all the states with masses $\gtrsim M_W$ and constructs the effective Hamiltonian of the form

$$\mathcal{H}_{\text{eff}} = \frac{G_F^2 M_W^2}{16\pi^2} \sum_X \lambda_{\text{CKM}}^X C_X \mathcal{O}_X, \quad (1)$$

where \mathcal{O}_X are the local four-quark operators (X labels different Lorentz structures: $X = \text{VLL, VRR, VLR, SLL, SRR, SLR, TL, and TR}$) and $\lambda_{\text{CKM}}^X C_X$ are their Wilson coefficients. An important feature of the minimal flavour violation is the factorisation of the Wilson coefficients into λ_{CKM}^X which depends only on the CKM matrix elements and C_X which to (a good approximation) are real numbers.

At the level of the effective Hamiltonian (1) models of new physics in which the CKM matrix is the only source of flavour and CP violation in the quark sector can be further divided into two broad classes [6]:

- The MFV (minimal flavour violation) models — truly minimal ones, in which, just as in the SM, only C_{VLL} Wilson coefficient is non-negligible and C_{VLL} responsible for $B_{s,d}^0-\bar{B}_{s,d}^0$ and $K^0-\bar{K}^0$ meson mixing are all equal (universal value of C_{VLL}).
- The GMFV (generalised minimal flavour violation) models — in which more C_X are non-negligible and/or are non-universal.

As we shall see, the MSSM can be of either type, depending on the ratio $v_2/v_1 \equiv \tan \beta$ of the vacuum expectation values of the two Higgs boson doublets.

Basic formulae used to determine $\bar{\rho}$ and $\bar{\eta}$ read (see *e.g.* Refs. [6, 7] for further details):

$$\bar{\eta} [(1 - \bar{\rho})A^2\eta_2 F^\varepsilon + P_c] A^2 \hat{B}_K = 0.204, \quad (2)$$

where the number on the r.h.s. stems from the measured value $\varepsilon_K = 2.28 \times 10^{-3}$, and

$$\begin{aligned} \Delta M_d &= \frac{G_F^2 M_W^2}{16\pi^2} M_{B_d} \eta_B \hat{B}_{B_d} F_{B_d}^2 |V_{tb}^* V_{td}|^2 |F^d| \propto \hat{B}_{B_d} F_{B_d}^2 |(1 - \bar{\rho}) - i\bar{\eta}|^2 |F^d|, \\ \Delta M_s &= \frac{G_F^2 M_W^2}{16\pi^2} M_{B_s} \eta_B \hat{B}_{B_s} F_{B_s}^2 |V_{tb}^* V_{ts}|^2 |F^s| \propto \hat{B}_{B_s} F_{B_s}^2 F^s. \end{aligned} \quad (3)$$

In Eqs. (2), (3) $\eta_2 = 0.57$ and $\eta_B = 0.55$ summarise the short distance QCD corrections to C_{VLL} Wilson coefficients and $P_c = 0.30 \pm 0.05$ is the known charmed quark loop contribution to ε_K . Factors $\hat{B}_K \approx 0.85 \pm 0.15$, $\hat{B}_{B_d} F_{B_d}^2 \approx (230 \pm 40 \text{ MeV})^2$ and $\hat{B}_{B_s} F_{B_s}^2 \approx (265 \pm 40 \text{ MeV})^2$ [8] parameterising matrix elements of the standard VLL operators are the biggest sources of uncertainties. The three factors F^ε , F^d and F^s can be expressed in terms of the Wilson coefficients C_X , their QCD RG running and matrix elements of the operators \mathcal{O}_X for $X \neq \text{VLL}$. In a concrete model of new physics such as *e.g.* the MSSM, F^ε , F^d and F^s are calculable functions of its parameters¹. The distinction between MFV and GMFV models is reflected in that in the formers $F^\varepsilon = F^d = F^s$ whereas in the latter models all F^i can be different. In the SM $F^\varepsilon = F^d = F^s = F_{\text{SM}} = S_0(\bar{m}_t) \approx 2.38 \pm 0.11$ for $\bar{m}_t(m_t) = 166 \pm 5 \text{ GeV}$.

¹ All the matrix elements of the operators \mathcal{O}_X , also for $X \neq \text{VLL}$, are now known from lattice calculations [9, 10]. Nevertheless, the uncertainties in their values still introduce some uncertainty in the factors F^i which depend, apart from Wilson coefficients and calculable QCD RG factors, also on the ratios of these matrix elements to the matrix element of the standard VLL operator.

The measured $B_d^0-\bar{B}_d^0$ mass difference, $\Delta M_d = 0.496/\text{ps}$, puts the constraint² $1.04 \lesssim \sqrt{|F^d|}R_t \equiv \sqrt{|F^d|}|1 - \bar{\rho} - i\bar{\eta}| \lesssim 1.69$. The role of ΔM_s which does not depend directly on $\bar{\rho}$ and $\bar{\eta}$ is twofold. Firstly, as follows from Eqs. (3), any new physics model must be such that F^s it gives rise to satisfies [11]

$$0.52 \left(\frac{\Delta M_s}{15/\text{ps}} \right) < \left| \frac{F^s}{F_{\text{SM}}} \right| < 1.29 \left(\frac{\Delta M_s}{15/\text{ps}} \right). \quad (4)$$

Since at present only the lower limit on the $B_s^0-\bar{B}_s^0$ mass difference is known, $\Delta M_s > 15/\text{ps}$, the factor F^s is bounded only from below. Secondly, once measured, ΔM_s combined with ΔM_d will allow for more precise determination of $|V_{td}| \propto |1 - \bar{\rho} - i\bar{\eta}|$ because the ratio ξ^2 of $F_{B_s}^2 \hat{B}_{B_s}$ to $F_{B_d}^2 \hat{B}_{B_d}$ is known with better accuracy than these factors individually: $\xi = 1.15 \pm 0.06$ [13]. For given F^s/F^d , the value of R_t is then determined, from the formula

$$R_t \equiv |1 - \bar{\rho} - i\bar{\eta}| = 0.82 \xi \left(\frac{15/\text{ps}}{\Delta M_s} \right) \sqrt{\left| \frac{F^s}{F^d} \right|}.$$

Note that R_t determined in this way is universal in the whole class of MFV models for which $F^s/F^d = 1$. In contrast, in GMFV models the extracted value of R_t does depend on new physics contributions to F^s and/or F^d .

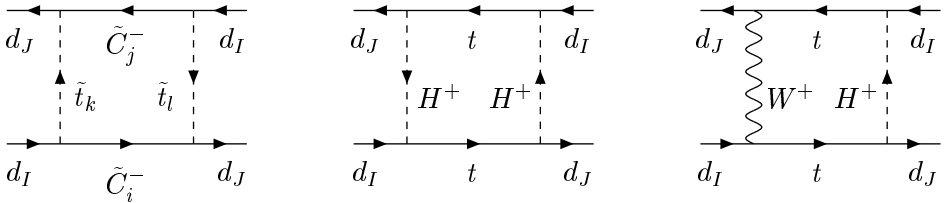


Fig. 1. Contribution of the chargino-stop and charged Higgs (W^\pm) boson box diagrams to F^ϵ , F^d and F^s in the MSSM. Crossed diagrams are not shown.

3. Supersymmetric contributions to F^ϵ , F^s and F^d

Dominant supersymmetric contributions to F^ϵ , F^s and F^d for small and moderate values of the ratio of the two MSSM Higgs boson doublets vacuum expectation values $v_2/v_1 \equiv \tan\beta$ are well studied [14, 15]. They arise from

² All bounds and allowed ranges of various quantities quoted in this article are obtained by scanning over all uncertainties within their respective 1σ ranges.

box diagrams shown in Fig. 1 and for $2 \lesssim \tan \beta \lesssim 20$ give $F^\varepsilon = F^d = F^s \equiv F$. Thus, for not too large values of $\tan \beta$ the MSSM is of the MFV type. Maximal values $F/F_{\text{SM}} \gtrsim 1.4$ are reached for lightest sparticles still not excluded by direct supersymmetry searches and $\tan \beta$ as small as possible³. With increasing $\tan \beta$ and/or increasing sparticle and charged Higgs boson masses the value of F/F_{SM} decreases to 1 [14, 15].

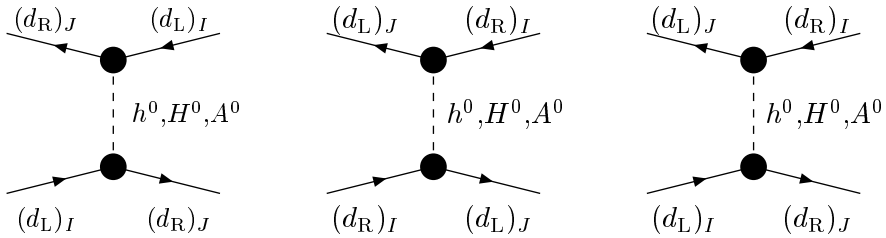


Fig. 2. Double penguin diagram contributing to C_1^{SLL} , C_1^{SRR} and C_2^{LR} Wilson coefficients, respectively in the MSSM with large $\tan \beta$.

As has been found recently [11, 16, 17] (see also [12]), for large values of $\tan \beta$, ~ 50 , the Wilson coefficient C_{SLL} , C_{SRR} and C_{SLR} of the effective Hamiltonian (1) can receive very large contributions from the so-called double scalar penguin diagrams (formally two-loop) shown in Fig. 2. The origin of the flavour changing couplings of the neutral Higgs bosons can be easiest understood in the effective Lagrangian approach [16, 18, 19] (see also [20]): due to the triangle (scalar penguin) diagram shown in Fig. 3(a), integrating out sparticles (but not the Higgs bosons) in the approximation of unbroken electroweak symmetry generates the Yukawa coupling of the H^u Higgs doublet to down-type quarks that is not present in the original MSSM Lagrangian. Thus, in the low energy effective Lagrangian both Higgs doublets, H^d and H^u , couple to down-type quarks and this, after the electroweak symmetry breaking, gives rise to the tree level flavour changing couplings of A^0 , h^0 and H^0 .

For the transitions $d_I \bar{d}_J \leftrightarrow d_J \bar{d}_I$ the double penguin diagrams give

$$C^{\text{SLL}} = -\frac{\alpha_{\text{em}}}{4\pi s_W^2} \frac{m_t^4}{M_W^4} m_{d_J}^2 X_{tC}^2 \tan^4 \beta \times \left(\frac{\cos^2 \alpha}{M_H^2} + \frac{\sin^2 \alpha}{M_h^2} - \frac{\sin^2 \beta}{M_A^2} \right),$$

$$C^{\text{SLR}} = -\frac{\alpha_{\text{em}}}{2\pi s_W^2} \frac{m_t^4}{M_W^4} m_{d_J} m_{d_I} X_{tC}^2 \tan^4 \beta \times \left(\frac{\cos^2 \alpha}{M_H^2} + \frac{\sin^2 \alpha}{M_h^2} + \frac{\sin^2 \beta}{M_A^2} \right).$$

³ Recall also, that for the top squarks lighter than 1 TeV in the range $1 \lesssim \tan \beta \lesssim 2$ is excluded by the unsuccessful search of the lightest Higgs boson at LEP.

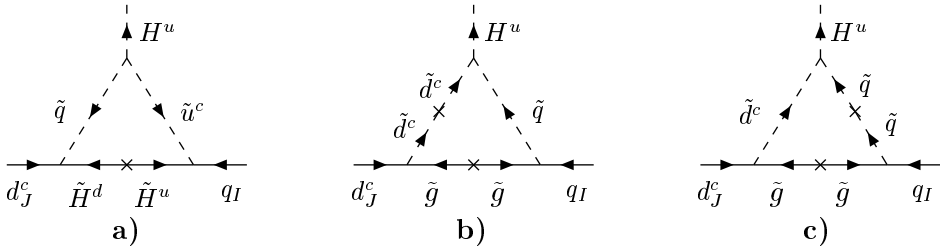


Fig. 3. Diagrams generating flavour changing neutral Higgs boson couplings. \tilde{q} , \tilde{u}^c and \tilde{d}^c denote electroweak eigenstates. Diagrams b) and c) contribute only in the case of non-minimal flavour violation arising from squark mass matrices (Sec. 5).

(C^{SRR} is obtained from C^{SLL} by replacing $m_{d_j}^2$ by $m_{d_l}^2$.) X_{tC} is given by

$$X_{tC} = \sum_{j=1}^2 Z_+^{2j} Z_-^{2j} \frac{A_t}{m_{C_j}} H_2(x_1^{t/C_j}, x_2^{t/C_j}),$$

where $x_i^{t/C_j} = M_{t_i}^2/m_{C_j}^2$, $i, j = 1, 2$ are the ratios of the stop and chargino masses squared, the matrices Z_+ and Z_- are defined in Ref. [21] and

$$H_2(x, y) = \frac{x \ln x}{(1-x)(x-y)} + \frac{y \ln y}{(1-y)(y-x)}.$$

Because for $M_A > M_Z$ and $\tan\beta \gg 1$ one has $M_H^2 \approx M_A^2$, $\sin\alpha \approx 0$, the coefficients C^{SLL} and C^{SRR} are suppressed [17]. It turns out however, that for sufficiently large stop mixing parameter A_t the double penguin contribution to C^{SLR} for the $b\bar{s} \leftrightarrow s\bar{b}$ transition is significant despite the suppression by the strange quark mass. Inserting numbers one finds

$$C^{\text{SLR}} \approx -4.64 \times \left(\frac{200 \text{ GeV}}{M_A}\right)^2 \left(\frac{\tan\beta}{50}\right)^4 X_{tC}^2$$

for $m_b = 2.7 \text{ GeV}$, $m_s = 60 \text{ MeV}$ at the scale $Q = m_t$, $M_H = M_A$ and $\sin\alpha = 0$. For $\tan\beta \sim 50$, $X_{tC} \sim \mathcal{O}(1)$ and CP-odd Higgs boson not too heavy this is comparable with the value of the Wilson coefficient of the standard VLL operator: $C^{\text{VLL}} = 4S_0(\bar{m}_t) \approx 9.5$. The ratio $C^{\text{SLR}}/C^{\text{VLL}}$ is further increased by the QCD RG effects [22]: $C^{\text{SLR}}(4.6 \text{ GeV}) = 2.23 C^{\text{SLR}}(m_t)$ while $C^{\text{VLL}}(4.6 \text{ GeV}) = 0.84 C^{\text{VLL}}(m_t)$. For the transitions $b\bar{d} \leftrightarrow d\bar{b}$ and $d\bar{s} \leftrightarrow s\bar{d}$ similar double penguin contributions to C^{SLR} are negligible being suppressed by $m_d/m_s \approx 0.06$ and $m_d/m_b \approx 0.001$, respectively. Thus, for large values of $\tan\beta$ the MSSM becomes of the GMFV type with $F^\varepsilon \approx F^d \approx F_{\text{SM}} \neq F^s$ and $F^s/F_{\text{SM}} < 1$.

The important features of the double penguin contribution to C^{SLR} are the following: it grows as $\tan^4 \beta$, it is always negative leading to $F^s < F_{\text{SM}}$ and is directly sensitive to the top squarks mixing ($C^{\text{SLR}} \propto A_t$). Moreover it does not vanish if all the sparticle mass parameters are uniformly scaled up (non-decoupling effect). It does however vanish as the inverse square of the Higgs sector mass scale set by M_A .

Figure 4 showing constraints from different experimental data in the $(\bar{\rho}, \bar{\eta})$ plane allows to discuss the value of V_{td} in the two scenarios: MSSM with small and large $\tan \beta$ as a function of measured in the future value of ΔM_s . ($R_t \propto |V_{td}|$ equals the length of the line connecting a given point in the $(\bar{\rho}, \bar{\eta})$ plane with the point $(1, 0)$.)

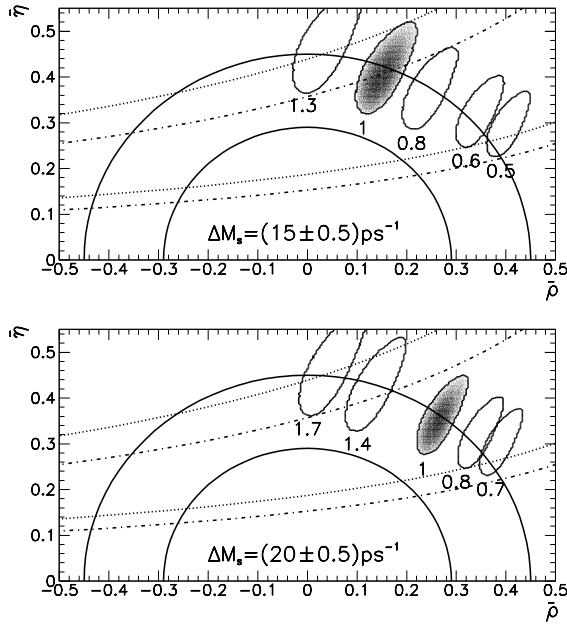


Fig. 4. Ranges of $(\bar{\rho}, \bar{\eta})$ allowed at 1σ for $\Delta M_s = (15.0 \pm 0.5)/\text{ps}$ (upper panel) and $(20.0 \pm 0.5)/\text{ps}$ (lower panel) for $\sin 2\beta_{\text{ut}} = 0.78 \pm 0.08$ and different values of F^s/F^d (marked in the figures). Black spots correspond to $F^s/F^d = 1$. Dotted (dash dotted) lines show the constraint on $(\bar{\rho}, \bar{\eta})$ from ϵ_K (Eq. (2)) for $F^\epsilon = F_{\text{SM}}$ (for $F^\epsilon = 1.3F_{\text{SM}}$ in the upper and for $F^\epsilon = 1.5F_{\text{SM}}$ in the lower panels, respectively) Solid semicircles mark the range of $R_b \equiv \sqrt{\bar{\rho}^2 + \bar{\eta}^2}$ allowed by $|V_{ub}/V_{cb}|$.

In the MFV-type MSSM with small $\tan \beta$, and also in the SM, $F^s/F^d = 1$ and $\bar{\rho}$ and $\bar{\eta}$ are bound to lie inside the black spots in figure 4 which are compatible (for $\sin 2\beta_{\text{ut}} \lesssim 0.78$) with the constraints imposed on R_b by the value of $|V_{ub}/V_{cb}|$. Therefore, V_{td} determined from $|V_{ub}/V_{cb}|$ ($\propto R_b$), $\Delta M_s/\Delta M_d$ ($\propto R_t$) and the asymmetry measured in the $B \rightarrow \psi K_S$ decay

($= \sin 2\beta_{\text{ut}}$) in the MFV-type MSSM and in the SM is the same: $|V_{td}| = (7.75\text{--}9.5) \times 10^{-3}$ ($R_t = 0.90\text{--}0.99$) for $\Delta M_s = (15 \pm 0.5)/\text{ps}$ and $|V_{td}| = (6.7\text{--}8.2) \times 10^{-3}$ ($R_t = 0.78\text{--}0.85$) for $\Delta M_s = (20 \pm 0.5)/\text{ps}$. Taking into account the constraint imposed on $\bar{\rho}$ and $\bar{\eta}$ by ε_K does not change anything for ΔM_s close to $20/\text{ps}$ (the shaded region lies entirely between the two ε_K hyperbolae even for $F^\varepsilon = 1.5$). On the other hand, if the value of ΔM_s is close to its present lower limit of $15/\text{ps}$, it follows from (4) that $F^\varepsilon = F^d = F^s$ must be smaller than ≈ 1.3 (MSSM parameters leading to F^ε bigger than 1.3 are excluded)⁴. Only for F^ε close to 1.3 can the upper edge of allowed R_t values (and therefore of $|V_{td}|$) determined from the fit to the data be slightly lower than in the SM. We conclude therefore that from the practical point of view the value of V_{td} in the SM and in the MFV type MSSM is the same. Note also, that in this scenario the factors $F_{B_s} \sqrt{\hat{B}_{B_s}}$ and $F_{B_d} \sqrt{\hat{B}_{B_d}}$ are positively correlated in the sense that, for fixed ΔM_s , bigger values of $F^\varepsilon = F^d = F^s$ require both these factors to assume simultaneously values from the lower parts of their respective ranges obtained from lattice calculations.

In the MSSM with $\tan\beta \sim 50$ $F^\varepsilon = F^d = F_{\text{SM}}$ and $F^s/F^d = F^s/F_{\text{SM}} < 1$. The absolute bound (4) does not allow for $|F^s/F^d| < 0.5$ for $\Delta M_s = 15/\text{ps}$ but the inspection of the upper panel of figure 4 shows that the combination of constraints imposed on $\bar{\rho}$ and $\bar{\eta}$ by ε_K (dotted lines) and R_b (solid semicircles) excludes also those MSSM parameters for which $|F^s/F^d| = |F^s/F_{\text{SM}}| \lesssim 0.55$. Similarly, for $\Delta M_s = 20/\text{ps}$ the bound (4) gives $|F^s/F^d| > 0.69$ whereas ε_K and R_b require $|F^s/F^d| \gtrsim 0.75$. For values of $|F^s/F^d|$ at the lower edge of the allowed range the value of $|V_{td}|$ extracted from $\Delta M_s/\Delta M_d$ is smaller than in the SM (for example, for $\Delta M_s = (15 \pm 0.5)/\text{ps}$ and $|F^s/F^d| = 0.6$ or for $\Delta M_s = (20 \pm 0.5)/\text{ps}$ and $|F^s/F^d| = 0.8$ $|V_{td}| = (6.0\text{--}7.3) \times 10^{-3}$). Note however, that for $-1 > F^s/F^d > -1.3$ for $\Delta M_s = (15 \pm 0.5)/\text{ps}$ ($-1 > F^s/F^d > -1.76$ for $\Delta M_s = (20 \pm 0.5)/\text{ps}$) the value of $|V_{td}|$ can be bigger than in the SM. Of course, large departures of $|F^s/F^d|$ from 1 discussed here are compatible with ΔM_s and ΔM_d separately provided the lattice factors $F_{B_s} \sqrt{\hat{B}_{B_s}}$ and $F_{B_d} \sqrt{\hat{B}_{B_d}}$ assume appropriate values (which however remain within their respective uncertainties). The correlation of $F_{B_s} \sqrt{\hat{B}_{B_s}}$ and $F_{B_d} \sqrt{\hat{B}_{B_d}}$ is again positive (although weaker than in the previous case): smaller $F^s/F^d = F^s/F_{\text{SM}}$ requires bigger $F_{B_s} \sqrt{\hat{B}_{B_s}}$ (to reproduce ΔM_s) and leads to smaller value of $|V_{td}|$ which in turn calls for bigger $F_{B_d} \sqrt{\hat{B}_{B_d}}$ to reproduce ΔM_d .

⁴ Note that this puts severe constraints on the scenario with $\tan\beta < 1$: stops, charginos and H^+ would have to be very heavy in order their contribution to $B_s^0\text{--}\bar{B}_s^0$ mixing described by F^s be sufficiently suppressed.

4. Impact of the scalar penguins

As has been pointed out in Ref. [23], the reliable calculation of the flavour changing neutral Higgs boson couplings in the MSSM requires resummation of the $\tan\beta$ enhanced terms. Furthermore, as demonstrated in Refs. [24,25] there are also $\tan\beta$ enhanced corrections to the couplings of the charged Higgs and Goldstone bosons which affect the box diagram contribution of these particles to the Wilson coefficients of the effective Hamiltonian (1). Technical details and systematic study of all these refinements can be found in [20] and will be not discussed here. They are however included in the numerical results presented below.

The role of the scalar penguin induced flavour changing neutral Higgs boson couplings is twofold. Firstly, for $\tan\beta \gtrsim 30$ a big portion of the MSSM parameter space (the bigger the higher is the lower experimental limit on ΔM_s) in which the parameter A_t is large (and hence the mixing of left and right top squarks is substantial) is excluded by the bound (4) and its refinement related to constraints on $\bar{\rho}$ and $\bar{\eta}$ from ε_K and $|V_{ub}/V_{cb}|$ discussed in the preceding section. Typical dependence of F^s/F_{SM} on the MSSM parameters is shown in figure 5. For $\mu > 0$ the resummation of $\tan\beta$ enhanced terms mentioned above increases [23] the value of F^s/F_{SM} (*i.e.* suppresses the negative contribution of the flavour changing couplings of neutral Higgs bosons) compared to the naive one-loop calculation of Ref. [11,26]. For $\mu < 0$, however, the effects of the flavour changing couplings are enhanced by the resummation. The parameters in figure 5 has been chosen so that μA_t has always the sign [25] which allows for cancellation of the tH^+ and chargino-stop contributions to the amplitude of the $\bar{B} \rightarrow X_s \gamma$ decay.

Secondly, the same flavour changing neutral Higgs boson couplings which (through the double penguin diagrams) affect the $B_s^0-\bar{B}_s^0$ mixing has been found [17,19,26] to totally dominate for $\tan\beta \gtrsim 30$ amplitudes of the decays $B_{s,d}^0 \rightarrow \mu^+ \mu^-$. Calculating the diagram shown in Fig. 6 one finds [19,26]

$$\mathcal{A}(B_q^0 \rightarrow \mu^+ \mu^-) = \bar{u}(k_1) (b + a\gamma^5) v(k_2), \quad (5)$$

where $q = s$ or d , $u(k_1)$, $v(k_2)$ are spinors of the final state leptons, and (without resummations, with $M_H \approx M_A$ *etc.*)

$$a = b = -V_{tb}^* V_{tq} m_t F_{B_q} \frac{G_F \alpha_{\text{em}}}{8\sqrt{2}s_W^2} \frac{M_{B_q}^2}{M_A^2} \frac{m_t^2}{M_W^2} X_{tC} \tan^3 \beta.$$

Therefore, in the MSSM with large $\tan\beta$ the decay rate behaves as $\text{BR}(B_{s,d}^0 \rightarrow \mu^+ \mu^-) \propto (\tan^6 \beta / M_A^4)$ and — without additional constraint imposed — could, for $\tan\beta \gtrsim 50$ and the Higgs bosons not too heavy, even

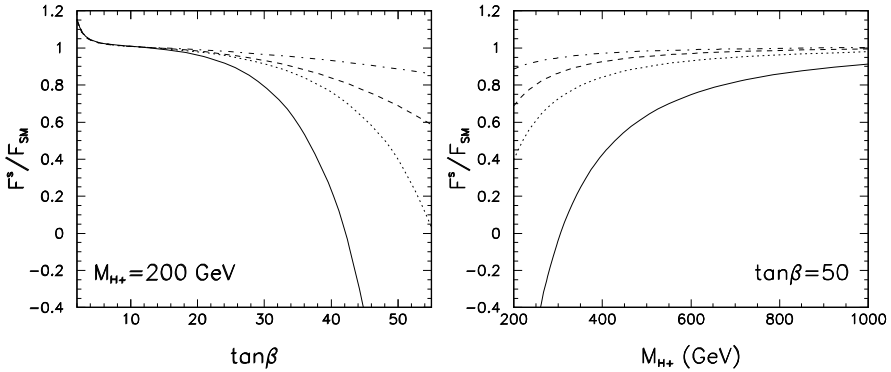


Fig. 5. F^s/F_{SM} as a function of $\tan\beta$ and M_{H^+} for the lighter chargino mass 750 GeV and $|M_2/\mu| = 1$. Solid and dashed lines correspond to stop masses (in GeV) (500, 850) whereas dotted and dot-dashed lines to (600, 750). The mixing angle between the two stops is $|\theta_{\bar{t}}| = 10^\circ$. Solid and dotted (dashed and dot-dashed) lines correspond to $\mu < 0$ ($\mu > 0$) and the stop mixing angle has the sign opposite to that of μ . $m_{\tilde{g}} = 3M_2$ and the right sbottom mass is 800 GeV.

exceed the present experimental bounds [5]

$$\begin{aligned} \text{BR}(B_s^0 \rightarrow \mu^+ \mu^-) &< 2.0 \times 10^{-6} \text{CDF}, \\ \text{BR}(B_d^0 \rightarrow \mu^+ \mu^-) &< 2.1 \times 10^{-7} \text{BaBar}. \end{aligned} \tag{6}$$

That is, the rates predicted in the MSSM could exceed by 3–4 orders of magnitude those of the SM [7,27,28]:

$$\begin{aligned} \text{BR}(B_s^0 \rightarrow \mu^+ \mu^-)_{SM} &\approx 3.5 \times 10^{-9} \left(\frac{F_{B_s}}{230 \text{ MeV}} \right)^2, \\ \text{BR}(B_d^0 \rightarrow \mu^+ \mu^-)_{SM} &\approx 1.4 \times 10^{-10} \left(\frac{F_{B_d}}{200 \text{ MeV}} \right)^2 \left(\frac{|V_{td}|}{0.009} \right)^2. \end{aligned}$$

However, as we have discussed above, for light A^0 the magnitude of the flavour changing scalar couplings $b_R A^0 s_L$ and $b_R H^0 s_L$ (and, hence, also of the couplings $b_R A^0 d_L$ and $b_R H^0 d_L$, because in the GMFV MSSM they are proportional to the former ones) is strongly constrained by the condition (4). Therefore one can expect that also the contribution of the neutral Higgs boson exchange shown in figure 6 to the amplitudes of the $B_{s,d}^0 \rightarrow \mu^+ \mu^-$ decays is bounded by the condition (4). In other words, the lower limit on ΔM_s should put the upper bound on the possible values of $\text{BR}(B_{s,d}^0 \rightarrow \mu^+ \mu^-)$ predicted in the MSSM.

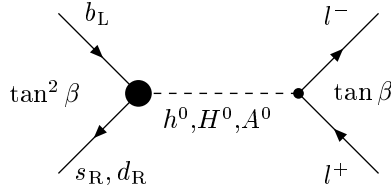


Fig. 6. Flavour changing neutral Higgs boson couplings contribution to the amplitude of the $B_{s,d}^0 \rightarrow l^+ l^-$ decays.

Figure 7, shows the correlation of the predicted values of $\text{BR}(B_{s,d}^0 \rightarrow \mu^+ \mu^-)$ and ΔM_s for a sample of the MSSM parameters for $M_A = 200$ GeV and $\tan \beta = 50$. In the case of the $\text{BR}(B_d^0 \rightarrow \mu^+ \mu^-)$ we have determined the value of $|V_{td}|$ consistently, that is we have scanned over the Wolfenstein parameters $\lambda, A, \bar{\rho}$ and $\bar{\eta}$ as well as over the nonperturbative parameters $F_{B_q} \sqrt{\hat{B}_{B_q}}$ and computed the rate only for those $\lambda, A, \bar{\rho}$ and $\bar{\eta}$ for which $\epsilon_K, \Delta M_d, \sin 2\beta_{\text{ut}}, |V_{ub}/V_{cb}|$ assumed acceptable values. We have also excluded all points for which the rate of the $\bar{B} \rightarrow X_s \gamma$ is unacceptable.

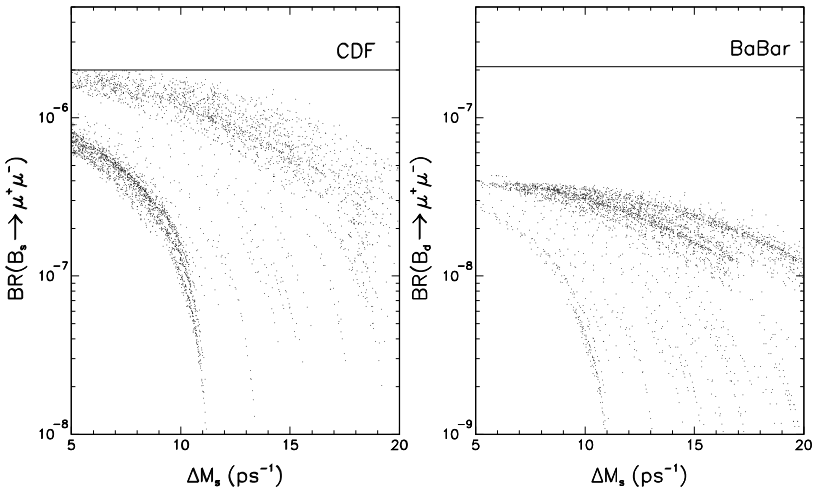


Fig. 7. Correlation of $\text{BR}(B_s^0 \rightarrow \mu^+ \mu^-)$ (left panel) and $\text{BR}(B_d^0 \rightarrow \mu^+ \mu^-)$ (right panel) with ΔM_s in the GMFV-type MSSM for $\tan \beta = 50$ and $M_A = 200$ GeV. In this case all points for which $F^s/F_{\text{SM}} < -0.52$ (so that $\Delta M_s > 15/\text{ps}$) give $\text{BR}(B_s^0 \rightarrow \mu^+ \mu^-)$ above the CDF bound (6) and have been discarded.

The upper bounds on $\text{BR}(B_{s,d}^0 \rightarrow \mu^+\mu^-)$ are clearly seen in figure 7. For $\tan\beta = 50$ and $M_A = 200$ GeV all points for which $F^s/F_{\text{SM}} < -0.52$ (so that $\Delta M_s > 15/\text{ps}$) give $\text{BR}(B_s^0 \rightarrow \mu^+\mu^-)$ above the CDF bound (6) and excluding also points for which $\Delta M_s < 15/\text{ps}$ we see, that $\text{BR}(B_s^0 \rightarrow \mu^+\mu^-) < 10^{-6}$ and $\text{BR}(B_d^0 \rightarrow \mu^+\mu^-) < 3 \times 10^{-8}$. Points for which $F^s/F_{\text{SM}} < -0.52$ can survive for smaller values of $\tan\beta$ and/or heavier CP-odd scalar A^0 (note that $\text{BR} \propto \tan^6\beta/M_A^4$ whereas $\Delta M_s \propto |F^s| \propto \tan^4\beta/M_A^2$). In this case however both, ΔM_s and $\text{BR}(B_{s,d}^0 \rightarrow \mu^+\mu^-)$ are entirely dominated by the contributions of the scalar penguins and it is easy to estimate that whenever $\text{BR}(B_s^0 \rightarrow \mu^+\mu^-)$ is below the CDF bound (6), $\text{BR}(B_d^0 \rightarrow \mu^+\mu^-) \lesssim 6 \times 10^{-8}$, *i.e.* it is below the BaBar bound (6).

We conclude that the MSSM parameter space in which the parameter A_t is not unnaturally big (that is, $A_t \lesssim M_{\text{SUSY}}$) is more strongly constrained by the lower limit on ΔM_s than by the non-observation of the $B_{s,d}^0 \rightarrow \mu^+\mu^-$ decays in CDF and BaBar. In particular the bound $\text{BR}(B_d^0 \rightarrow \mu^+\mu^-) < 3 \times 10^{-8}$ holds. For parameters such that $F^s/F_{\text{SM}} < -0.52$ (larger A_t) there is a weaker upper bound $\text{BR}(B_d^0 \rightarrow \mu^+\mu^-) \gtrsim 6 \times 10^{-8}$.

5. Flavour violation in squark mass matrices

In supersymmetric extension of the SM, flavour and CP violation can originate also in the sfermion sector. In general, the 6×6 mass squared matrices of left- and right-chiral sfermions of the same electric charge have the form⁵

$$\mathcal{M}_Q^2 = \begin{pmatrix} (M_{\text{LL}}^Q)^2 & (M_{\text{LR}}^Q)^2 \\ (M_{\text{RL}}^Q)^2 & (M_{\text{RR}}^Q)^2 \end{pmatrix} \quad Q = U, D, L,$$

where $(M_{\text{LL}}^Q)^2$ *etc.* are 3×3 submatrices. If the latter are not diagonal in the so-called superCKM basis, in which quark mass matrices are diagonal, then their off-diagonal entries generate flavour changing neutral currents. For example, large, $\propto \alpha_s^2$, contributions to $K^0-\bar{K}^0$ or $B_{s,d}^0-\bar{B}_{s,d}^0$ mixing are then induced by the gluino box diagrams shown in figure 8. In this figure the off-diagonal entries of matrices $(M_{XY}^Q)^2$ are treated as additional interactions (the so-called mass insertion approximation [15, 29, 30]). As these contributions are not proportional to the CKM matrix factors the effective Hamiltonian (1) for $|\Delta F| = 2$ transitions has to be now written as

$$\mathcal{H}_{\text{eff}} = \sum_X C_X \mathcal{O}_X,$$

⁵ Except for sneutrinos whose mass squared matrix consists of the LL 3×3 block only.

where C_X are the Wilson coefficients computed in the MSSM and \mathcal{O}_X are the same four-quark operators as in Eq. (1). Assuming for definiteness that sparticle masses are of the order of $M_{\text{SUSY}} = 500$ GeV, and taking into account the QCD RG running of C_X between M_{SUSY} and the hadronic scale as well as matrix elements of the operators \mathcal{O}_X between the meson states in the manner described in [22] one obtains for the supersymmetric contribution to the $K^0-\bar{K}^0$ transition amplitude:

$$\begin{aligned} \langle \bar{K}^0 | \mathcal{H}_{\text{eff}} | K^0 \rangle \approx & M_K F_K^2 [0.15 (C_{\text{SUSY}}^{\text{VLL}} + C_{\text{SUSY}}^{\text{VRR}}) - 6.0 (C_{\text{SUSY}}^{\text{SLL}} + C_{\text{SUSY}}^{\text{SRR}}) \\ & - 11.5 (C_{\text{SUSY}}^{\text{TL}} + C_{\text{SUSY}}^{\text{TR}}) - 13.84 C_{\text{SUSY}}^{\text{VLR}} + 22.48 C_{\text{SUSY}}^{\text{SLR}}], \end{aligned} \tag{7}$$

where we have used $\alpha_s(M_Z) = 0.1185$. The large numerical factors⁶ in the second line originate from the RG running and from the chiral enhancement factor $(M_K/(m_s+m_d))^2 \approx 18$ for $m_s(2 \text{ GeV}) = 110 \text{ MeV}$. For the supersymmetric contribution to the $B_q^0-\bar{B}_q^0$ transition amplitude one has to replace in Eq. (7) $M_K F_K^2$ by $M_{B_q} F_{B_q}^2$ ($q = d$ or s) and the numbers in the square bracket by: 0.24, -0.49 , -0.94 , -0.97 and 1.27, respectively. Note, that there is no chiral enhancement in this case as $(M_{B_q}/(m_b+m_d))^2 \approx 1.65$.

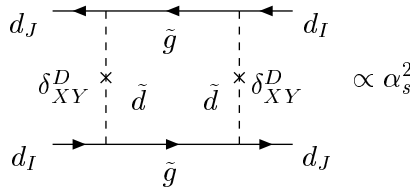


Fig. 8. Contribution of gluino-squark box diagrams neutral meson mixing. Crosses denote mass insertions.

Using the standard formulae

$$\begin{aligned} \Delta M_K &= 2 \text{Re} \langle \bar{K}^0 | \mathcal{H}_{\text{eff}} | K^0 \rangle, \\ \varepsilon_K &= \frac{e^{i\pi/4}}{\sqrt{2}\Delta M_K} \text{Im} \langle \bar{K}^0 | \mathcal{H}_{\text{eff}} | K^0 \rangle, \\ \Delta M_q &= 2 |\langle \bar{B}_q^0 | \mathcal{H}_{\text{eff}} | B_q^0 \rangle| \end{aligned}$$

⁶ Some uncertainties of order few percent in these numbers are due to the uncertainties of the B_K^X factors parameterising matrix elements of the operators \mathcal{O}_X for X=SLL, SRR, VLR, SLR, TL, TR. [9]

and plugging in numbers one finds

$$\begin{aligned}
 \Delta M_K &= 3.87 \times 10^4 \operatorname{Re} (M_{\tilde{q}}^2 \times [\dots]) \left(\frac{1 \text{ TeV}}{M_{\tilde{q}}^2} \right)^2 \text{ ps}^{-1}, \\
 \varepsilon_K &= -2.58 \times 10^6 \operatorname{Im} (M_{\tilde{q}}^2 \times [\dots]) \left(\frac{1 \text{ TeV}}{M_{\tilde{q}}^2} \right)^2 e^{i\pi/4}, \\
 \Delta M_d &= 6.45 \times 10^5 \operatorname{Re} (M_{\tilde{q}}^2 \times [\dots]) \left(\frac{1 \text{ TeV}}{M_{\tilde{q}}^2} \right)^2 \text{ ps}^{-1}, \\
 \Delta M_s &= 8.78 \times 10^5 \operatorname{Re} (M_{\tilde{q}}^2 \times [\dots]) \left(\frac{1 \text{ TeV}}{M_{\tilde{q}}^2} \right)^2 \text{ ps}^{-1}, \quad (8)
 \end{aligned}$$

where $M_{\tilde{q}}^2$ is some average mass of squarks and $[\dots]$ denote the content of square brackets from Eq. (7) appropriate for a given transition.

In the lowest order in the mass insertion approximation each of the Wilson coefficients C_X for $|\Delta F| = 2$ transitions like $K^0-\bar{K}^0$ and $B_q^0-\bar{B}_q^0$ can be represented as a product of a function of $M_{\tilde{q}}^2$ and $m_{\tilde{g}}$ and of two mass insertions defined as [15, 29, 30]

$$(\delta_{XY}^D)^{JI} = \frac{[(M_{XY}^D)^2]^{JI}}{M_{\tilde{q}}^2},$$

where $X, Y = \text{L,R}$, and the indices J, I label generations. Neglecting contributions other than those generated by gluino exchanges, one has

$$\begin{aligned}
 C_{\text{SUSY}}^{\text{VLL}} &= a \alpha_s^2 [(\delta_{\text{LL}}^D)^{JI}]^2, & C_{\text{SUSY}}^{\text{VRR}} &= b \alpha_s^2 [(\delta_{\text{RR}}^D)^{JI}]^2, \\
 C_{\text{SUSY}}^{\text{SLR}} &\propto \alpha_s^2 [a' (\delta_{\text{LL}}^D)^{JI} (\delta_{\text{RR}}^D)^{JI} + b' (\delta_{\text{LR}}^D)^{JI} (\delta_{\text{RL}}^D)^{JI}] \quad (9)
 \end{aligned}$$

etc. [30], where $JI = 21, 31$ and 32 for $K^0-\bar{K}^0$, $B_d^0-\bar{B}_d^0$ and $B_s^0-\bar{B}_s^0$ transitions, respectively.

Comparison of the numbers in Eqs. (8) with the experimental values: $\Delta M_K = 0.0053/\text{ps}$, $\varepsilon_K = 2.28 \times 10^{-3}$ and $\Delta M_d = 0.496/\text{ps}$ illustrates the so-called supersymmetric flavour and CP problem: taking into account that the dimensionless factors $M_{\tilde{q}}^2 \times [\dots]$ in Eqs. (8) are $\sim \mathcal{O}(1)$, it is clear that the typical contribution to ΔM_K , ε_K , ΔM_{B_q} and to many other measured quantities like ε'/ε , $\text{BR}(\bar{B} \rightarrow X_s \gamma)$ [15, 31, 32], *etc.* in the MSSM with the flavour and CP violation in squark mass matrices is several orders of magnitude too big. Any theory of supersymmetry breaking has to face the problem of explaining the smallness of the mass insertions δ_{XY}^Q .

Adopting the rough criterion that the gluino contribution alone to $|\Delta M_K|$ and $|\varepsilon_K|$ should not exceed the experimental values of these quantities (and barring possible cancellation between different mass insertions) one obtains for small and moderate values of $\tan\beta$ the limits shown in the middle column of Table I. For comparison in the first column we show the limits obtained in the paper [30]. The differences stem from slightly different treatment of the NLO QCD RG evolution and of the matrix elements of the operators involved (our approach is based on Ref. [22]) but are inessential for the order of magnitude estimates of the limits.

TABLE I

Upper limits on mass insertions obtained from ε_K for $M_{\tilde{g}} = 500$ GeV. The limits scale approximately as $M_{\tilde{q}}^2$. $x \equiv (m_{\tilde{q}}/M_{\tilde{q}})^2$. Limits on $[(\delta_{12}^D)_{\text{RR}}^2]$ are the same as for $[(\delta_{12}^D)_{\text{LL}}^2]$. As follows from numbers in the first two of Eqs. (8), the corresponding limits on real parts of the product of insertions are simply 12.5 times weaker than those given below. (This simple rule is not satisfied by the numbers quoted in Ref. [30].)

	Ref. [30]	\tilde{g} low $\tan\beta$	\tilde{g} $\tan\beta = 50$
x	$\sqrt{ \text{Im} [(\delta_{12}^D)_{\text{LL}}^2] }$		
0.3	2.9×10^{-3}	2.7×10^{-3}	2.5×10^{-3}
1.0	6.1×10^{-3}	6.0×10^{-3}	1.7×10^{-3}
4.0	1.4×10^{-2}	1.5×10^{-2}	2.0×10^{-3}
9.0	—	1.4×10^{-2}	2.4×10^{-3}
x	$\sqrt{ \text{Im} [(\delta_{12}^D)_{\text{LR}}^2] }$	$(\delta_{12}^D)_{\text{LR}} \gg (\delta_{12}^D)_{\text{RL}})$	
0.3	3.4×10^{-4}	2.5×10^{-4}	2.2×10^{-4}
1.0	3.7×10^{-4}	2.9×10^{-4}	2.2×10^{-4}
4.0	5.2×10^{-4}	4.2×10^{-4}	2.5×10^{-4}
4.0	—	6.5×10^{-4}	6.9×10^{-4}
x	$\sqrt{ \text{Im} [(\delta_{12}^D)_{\text{LL}}(\delta_{12}^D)_{\text{RR}}] }$		
0.3	1.1×10^{-4}	8.2×10^{-5}	8.0×10^{-5}
1.0	1.3×10^{-4}	9.5×10^{-5}	9.2×10^{-5}
4.0	1.8×10^{-4}	1.4×10^{-4}	1.3×10^{-4}
9.0	—	1.9×10^{-4}	1.8×10^{-4}

It is interesting to note, that because ε_K puts stringent bounds only on imaginary parts of products of two mass insertions, bounds on almost real and almost imaginary mass insertions are provided only by ΔM_K and

are order of magnitude weaker, although such a conspiracy seems not very natural. Stronger absolute bound on the imaginary part of the mass insertion itself exist only for $(\delta_{LR}^D)^{12}$ and follows from ε'/ε : $|\text{Im}(\delta_{LR}^D)^{12}| \lesssim 10^{-5}$ [29,33].

For mass insertions generating transitions between the third and the first two generations of quarks only much weaker bounds are available. Limits on $(\delta_{XY}^D)^{13}$ insertions from the gluino box contribution to ΔM_d have been derived recently in Ref. [34]. Similar limits on $(\delta_{XY}^D)^{23}$ insertions will become available once ΔM_s is measured. At present however, stringent bounds from the $\bar{B} \rightarrow X_s \gamma$ decay exist only for the insertions $(\delta_{LR}^D)^{23}$ and $(\delta_{RL}^D)^{23}$: $|(\delta_{LR}^D)^{23}| < 0.07 \times (M_{\tilde{q}}/1 \text{ TeV})$. The remaining insertions are bounded rather weakly [15,32].

For large $\tan\beta$ the standard analysis of bounds on mass insertions derived from $|\Delta F| = 2$ transitions based on gluino box diagrams of figure 8 is not sufficient. Scalar flavour changing neutral Higgs boson couplings can generate additional contributions $\propto \tan^4 \beta$ to the Wilson coefficients C^{SLR} through the double penguin diagrams of figure 2 (contributions to C^{SLL} , and C^{SRR} Wilson coefficients are suppressed because of the mutual cancellation of H^0 and A^0 contributions) and these contributions have to be taken into account. Dominant source of the flavour changing neutral Higgs boson couplings in the case of flavour violation in squark mass matrices are the diagrams (b) and (c) shown in figure 3. Calculating those diagrams one gets the couplings

$$\mathcal{L} = S^0 \overline{d_R^J} [X_{RL}^S]^{JI} d_L^I + S^0 \overline{d_L^J} [X_{LR}^S]^{JI} d_R^I \quad J \neq I, \quad (10)$$

where the matrix coefficients $X_{RL}^S = (X_{LR}^S)^\dagger$ are given by

$$[X_{RL}^S]^{JI} = x_d^S \tan^2 \beta \frac{e\alpha_s}{3\pi s_W} \frac{m_{\tilde{g}} \mu^*}{M_{\tilde{q}}^2} \left[(\delta_{LL}^D)^{IJ} \frac{m_{d_J}}{M_W} + \frac{m_{d_I}}{M_W} (\delta_{RR}^D)^{IJ} \right] \times D(m_{\tilde{g}}^2, M_{\tilde{q}}^2)$$

with $x_d^S = \cos \alpha, -\sin \alpha$ and $i \sin \beta$ for $S^0 = H^0, h^0$ or A^0 , respectively and $D(a, b)$ some dimensionless function.

It turns out that even the limits on $(\delta_{LL}^D)^{12}$ and $(\delta_{RR}^D)^{12}$ mass insertions are affected by the double penguin contribution which is significantly enhanced by the big numerical factor multiplying $C_{\text{SUSY}}^{\text{SLR}}$ in Eq. (7). The effect of double penguin contribution is seen in Table I in the limits on imaginary (and real) parts of $[(\delta_{LL}^D)^{12}]^2$ and $[(\delta_{RR}^D)^{12}]^2$ which for $m_{\tilde{g}} > M_{\tilde{q}}$ become stronger by one order of magnitude compared to similar limits for lower $\tan\beta$ values. That the improvement is seen only for $m_{\tilde{g}} > M_{\tilde{q}}$ follows

from the fact that the couplings (10) are proportional to $m_{\tilde{g}}$. The limits on $(\delta_{LL}^D)^{12}(\delta_{RR}^D)^{12}$ are not improved because, as is clear from Eq. (9), the gluino box contribution to $C_{\text{SUSY}}^{\text{SLR}}$ contains already a term proportional to $(\delta_{LL}^D)^{12}(\delta_{RR}^D)^{12}$.

In the same manner, bounds on the insertions $(\delta_{LL}^D)^{13}$ and $(\delta_{RR}^D)^{13}$ (and when ΔM_s is measured also on $(\delta_{LL}^D)^{23}$ and $(\delta_{RR}^D)^{23}$) derived from $B^0-\bar{B}^0$ mixing [34] should also be modified for large values of $\tan\beta$. We have found, however, that the actual bounds depend also the chargino box and double penguin contributions and can not be therefore presented in a simple way.

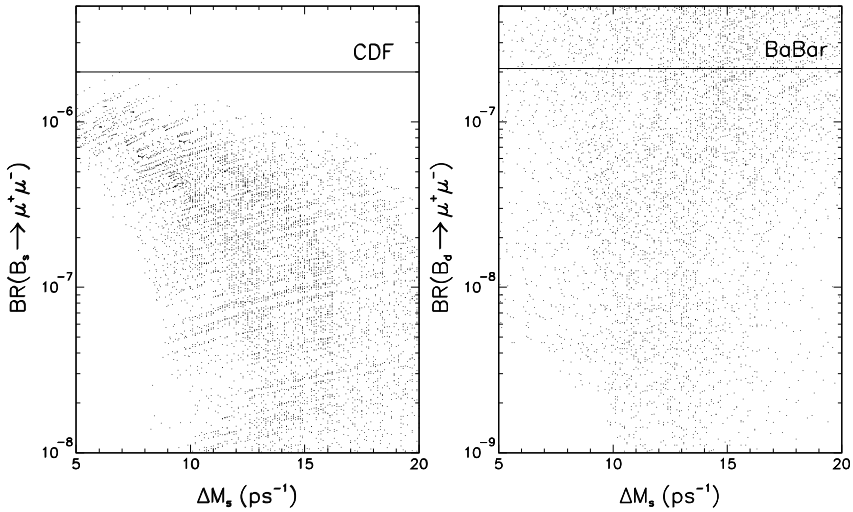


Fig. 9. Correlation of $\text{BR}(B_s^0 \rightarrow \mu^+\mu^-)$ (left panel) and $\text{BR}(B_d^0 \rightarrow \mu^+\mu^-)$ (right panel) with ΔM_s in the MSSM with flavour violation in the squark sector. The single nonzero mass insertion $(\delta_{LL}^D)^{31}$ has been varied in the range (0.01, 0.1). $\tan\beta = 50$ and $M_A = 200$ GeV.

Another interesting effect related to the flavour changing couplings (10) generated for large $\tan\beta$ by non-zero LL and/or RR mass insertions is a growing like $\tan^6\beta$ contribution to the amplitudes of $B_s^0 \rightarrow \mu^+\mu^-$ and/or $B_d^0 \rightarrow \mu^+\mu^-$ decays [19]. Calculating the contribution of the diagram shown in figure 6 with the couplings (10) one finds for the coefficients a in the amplitude (5)

$$a = F_{B_q} m_l \frac{e^2 \alpha_s}{12\pi s_W^2 M_W^2} \frac{M_B^2}{M_A^2} \tan^3 \beta \left[\frac{m_{\tilde{g}} \mu^*}{M_{\tilde{q}}^2} (\delta_{LL}^D)^{3q} + \frac{m_{\tilde{g}} \mu}{M_{\tilde{q}}^2} (\delta_{RR}^D)^{3q} \right] \times D(m_{\tilde{g}}^2, M_{\tilde{q}}^2),$$

where $q = d = 1$ and $q = s = 2$ for B_d^0 and B_s^0 decays, respectively, and the coefficient b in the amplitude (5) is given by the similar expression with $+$ changed to $-$ in the square bracket. It has been shown [19], that for $\tan\beta \sim 50$, $M_A \gtrsim 200$ GeV and with mass insertions of order 0.1 the branching ratios predicted in the MSSM can exceed by one or two orders of magnitude the present experimental limits (6). It is however important to check whether this remains true when all the available constraints are respected, including the ones imposed by ΔM_s and ΔM_d and taking consistently into account the double penguin contributions to these quantities. The results of this exercise are shown in figure 9 where we show the branching ratios of the decays $B_s^0 \rightarrow \mu^+\mu^-$ and $B_d^0 \rightarrow \mu^+\mu^-$ versus the mass difference ΔM_s for a sample of the MSSM parameters varying the insertion $(\delta_{LL}^D)^{31}$ in the range (0.01, 0.1). All points giving rise to experimentally unacceptable values of ΔM_d and/or $\text{BR}(\bar{B} \rightarrow X_s\gamma)$ have been discarded. Points for which $F^s < 0$ have been discarded as well. Since we set the insertions $(\delta_{LL}^D)^{32}$ and $(\delta_{RR}^D)^{32}$ equal to zero the increase of $\text{BR}(B_s^0 \rightarrow \mu^+\mu^-)$ compared to the SM prediction seen in the left panel of figure 9 is mainly due to the effects discussed in Section 4.

It is clear from figure 9 that even with all the cuts imposed the possible values of the branching ratio $\text{BR}(B_d^0 \rightarrow \mu^+\mu^-)$ can still be above the present experimental limit (6) which means that the non-observation of the $B_d^0 \rightarrow \mu^+\mu^-$ decay imposes nontrivial constraints on the MSSM parameter space and on the mass insertions $(\delta_{LL}^D)^{31}$ and $(\delta_{RR}^D)^{31}$.

Finally, comparison the possible effects in the MSSM without and with flavour violation in the squark mass matrices (figures 7 and 9, respectively) leads to the interesting conclusion that, within the supersymmetric framework, observation of the $B_d^0 \rightarrow \mu^+\mu^-$ decay at the level close to the present BaBar limit (6) (*i.e.* with BR above $\sim 6 \times 10^{-8}$ in general and above $\sim 3 \times 10^{-8}$ if unnaturally large and very unlikely values of the stop mixing parameters A_t are not taken into account), apart for implying that the scale of the Higgs sector is not far from the electroweak scale, would be a very strong evidence of non-minimal flavour violation in the quark sector.

6. Effects of flavour violation in the lepton sector

To complete the picture of flavour violation in the supersymmetric extension of the SM model we discuss briefly also the lepton sector.

To account for the observed atmospheric and solar neutrino oscillations [36] the analog of the CKM mixing matrix, the so-called Maki–Nakagawa–Sakata mixing matrix [35], has to be introduced in the leptonic sector of the SM or the MSSM. Under the assumption that the mixing occurs only between the three known neutrino flavours (no sterile neutrinos) which is

supported by the SNO results [37], the MNS matrix U is of dimension 3×3 and is usually parameterised in a similar way as the CKM matrix

$$U = \begin{pmatrix} c_{12}c_{13} & s_{12}c_{13} & s_{13} \\ \cdot & \cdot & s_{23}c_{13} \\ \cdot & \cdot & c_{23}c_{13} \end{pmatrix}, \quad (11)$$

where $c_{12} = \cos \theta_{12}$ *etc.* and where we show only the entries directly related to observed oscillations and neglected all possible CP violating phases. Non-zero angles θ_{12} and θ_{23} are responsible for solar and atmospheric neutrino oscillations, respectively.

The pattern of U emerging from the experimental data [38,39]

$$\begin{aligned} |U_{11}| &\approx |U_{12}| \approx \frac{1}{\sqrt{2}}, \\ |U_{23}| &\approx |U_{33}| \approx \frac{1}{\sqrt{2}}, \\ |U_{13}| &\approx 0 \end{aligned} \quad (12)$$

is called bi-maximal mixing and is distinctly different from the hierarchical pattern of the CKM matrix.

Nontrivial mixing matrix U (11) induces of course also flavour violating processes with charged leptons, such a $\mu \rightarrow e\gamma$ or $Z^0 \rightarrow e\mu$ *etc.* but at rates which are unmeasurably small (*e.g.* $\text{BR}(\mu \rightarrow e\gamma) < 10^{-50}$) for neutrino mass squared differences required to explain the SuperKamiokande data:

$$\begin{aligned} \Delta m_{\text{atm}}^2 &\equiv m_{\nu_3}^2 - m_{\nu_2}^2 \approx 3.2 \times 10^{-3} \text{ eV}^2, \\ \Delta m_{\text{sol}}^2 &\equiv m_{\nu_2}^2 - m_{\nu_1}^2 \sim \mathcal{O}(10^{-4}) \text{ eV}^2 \end{aligned}$$

and masses compatible with constraints imposed by cosmology ($\sum_a m_{\nu_a} < \text{few eV}$). Thus, if the MNS mixing matrix is the only source of flavour violation in the leptonic sector, neutrino oscillations remain the only observable lepton flavour violating phenomenon.

In supersymmetric extension of the SM lepton flavour violation can originate also in the slepton mass squared matrices. Existing experimental upper bounds: $\text{BR}(\mu \rightarrow e\gamma) < 10^{-11}$, $\text{BR}(\tau \rightarrow e(\mu)\gamma) < 10^{-6}$ put stringent constraint only on the mass insertion $|\delta_{\text{LR}}^l|^{12}$ which has to be smaller than 10^{-5} ; constraints on the other sleptonic mass insertions are of order of $\text{few} \times 10^{-1}$ [15].

Interesting links between the lepton flavour violation originating in the slepton sector and neutrino masses and mixing exist in the see-saw scenario in which observed small neutrino masses result from exchanges of right-handed neutrinos ν_{R} of masses $M_{\nu_{\text{R}}} \sim 10^{10} - 10^{14} \text{ GeV}$ in the GUT-type

framework. Firstly, the RG running of the parameters of the theory between the scales M_{GUT} and M_{ν_R} necessarily induces lepton flavour violating mass insertions. It turns out that the experimental limits on $\mu \rightarrow e\gamma$, $\tau \rightarrow e(\mu)\gamma$ decays put interesting constraints on realizations of the see-saw mechanism in the GUT-type scenarios [40]. Secondly, lepton flavour violating originating in the slepton sector can influence neutrino masses and mixing via quantum corrections below the scale M_{ν_R} . Let us discuss this point in some details.

Quantum corrections to neutrino masses and mixing below the M_{ν_R} scale are of two types. The first one are the corrections depending on $\ln(M_{\nu_R}/M_W)$ which are accounted for by integrating the renormalisation group equations [41] of the dimension 5 operator between the scales M_{ν_R} and M_W . The most interesting aspect of the RG equations is their fixed point structure [42]: whenever the RG running is substantial, the mixing angles evolve in such a way that at the M_W scale either $U_{31} = 0$ or $U_{32} = 0$. In both cases one gets the following relation between the mixing angles

$$\sin^2 2\theta_{12} = \frac{s_{13}^2}{(s_{23}^2 c_{13}^2 + s_{13}^2)^2} \sin^2 2\theta_{23}.$$

Because of the CHOOZ limit $s_{13}^2 < 0.16$ [39] this is incompatible with the bi-maximal mixing pattern (12) favoured by the solar and atmospheric neutrino data. This means that always for exact three-fold or two-fold degeneracy of neutrino masses at the scale M_{ν_R} , or for approximate degeneracies of neutrinos having the same CP parities, when the RG running is substantial [42], the mixing angles obtained from the see-saw mechanism are phenomenologically unacceptable. Note also that these are precisely the most interesting cases: three-fold degeneracy of neutrinos will be required if the neutrinoless double beta decay is found at the level requiring $m_{\nu}^{ee} \sim 0.5$ eV. More generally, see-saw scenarios giving naturally large mixing angles may be easier to find if the spectrum of neutrino masses is (approximately) degenerate.

The unacceptable pattern of mixing generated by RG running can however be changed by the second type of quantum corrections to the neutrino mass matrix — the so-called low energy threshold corrections — if there is some lepton flavour violation in the slepton sector [43].

In the basis in which the neutrino mass matrix $(\mathbf{m}_{\nu}^0)^{AB}$ generated by the underlying see-saw mechanism is diagonal the corrected neutrino mass matrix can be written as [45, 46]

$$m_{\nu_a}^{(0)} \delta^{ab} + \left[U^T \left(\mathbf{I}^T \mathbf{m}_{\nu}^{(0)} + \mathbf{m}_{\nu}^{(0)} \mathbf{I} \right), U \right]^{ab}, \quad (13)$$

where U is the uncorrected MNS matrix and

$$\mathbf{I}^{AB} = \mathbf{I}_{\text{th}}^{AB} - \delta^{AB} \mathbf{I}_{\text{rg}}^A \quad (14)$$

summarises the RG (\mathbf{I}_{rg}^A) and low energy threshold ($\mathbf{I}_{\text{th}}^{AB}$) corrections. The most interesting part of the latter corrections take the form [45]

$$\mathbf{I}_{\text{th}}^{AB} \approx \left(\delta_{\text{LL}}^l\right)^{AB} \times f(M_I^2, m_C^2),$$

where the function of chargino and slepton masses f is typically of order $\text{few} \times (10^{-4} - 10^{-3})$ (contributions of δ_{RR}^l and δ_{LR}^l to $\mathbf{I}_{\text{th}}^{AB}$ are smaller). For comparison, for $M_{\nu_R} \sim 10^{10}$ GeV, $\mathbf{I}_{\text{rg}}^\tau \approx 10^{-5} \times \tan^2 \beta$, and $\mathbf{I}_{\text{rg}}^\mu, \mathbf{I}_{\text{rg}}^e$ are negligible.

In the case of the (approximate) degeneracy of the zeroth order neutrino masses $m_{\nu_a}^{(0)} \approx m_{\nu_b}^{(0)}$ the matrix U is fixed by the condition

$$\sum_{AB} U_{Aa} \mathbf{I}_{AB} U_{Bb} = 0 \tag{15}$$

(the freedom $U \rightarrow U \cdot R_{ab}$, where R_{ab} is an arbitrary rotation of the ν_a and ν_b neutrino fields, is used to diagonalise the ‘‘perturbation’’). This leads to the fixed point-like relations between the mixing angles which are different than the RG evolution provided $|\mathbf{I}_{\text{th}}^{AB}| \gtrsim |\mathbf{I}_{\text{rg}}^A|$ [43].

As an example consider initial degeneracy of the three neutrinos $m_{\nu_a} \approx m_{\nu_b} \approx -m_{\nu_c}$ and only one dominant correction $\mathbf{I}_{\text{th}}^{AB}$. In this case interesting results are obtained for $m_{\nu_1} \approx m_{\nu_3}$ (or $m_{\nu_2} \approx m_{\nu_3}$) and dominant $\mathbf{I}_{\text{th}}^{\mu\tau}$ correction (*i.e.* $(\delta_{\text{LL}}^l)^{23} \neq 0$). The condition (15) then gives

$$s_{13} = -\cot 2\theta_{23} \tan \theta_{12} (\cot \theta_{12})$$

which is compatible with the bi-maximal mixing and small $U_{13} = s_{13}$ element. Moreover, for the mass squared differences one obtains

$$\begin{aligned} \Delta m_{\text{sol}}^2 &= -4m_\nu^2 \cos 2\theta_{12} \sin 2\theta_{23} \mathbf{I}_{\text{th}}^{\mu\tau} \\ \Delta m_{\text{atm}}^2 &= -4m_\nu^2 (1 + \cos^2 \theta_{12}) \sin 2\theta_{23} \mathbf{I}_{\text{th}}^{\mu\tau} \end{aligned}$$

that is, for the bi-maximal mixing:

$$\Delta m_{32}^2 \gg \Delta m_{21}^2 \sim 0$$

in agreement with the experimental information. $\Delta m_{\text{atm}}^2 \approx 3 \times 10^{-3} \text{ eV}^2$ requires then $m_\nu \approx 1 \text{ eV}^2$ and $(\delta_{\text{LL}}^l)^{23} \sim 0.5$ with the interesting implications for the $\tau \rightarrow \mu\gamma$ decay. Δm_{sol}^2 of right magnitude can be generated either by departure from $\theta_{12} = \pi/4$ or, by another, hierarchically smaller, correction: flavour conserving $\mathbf{I}^{AB} = \mathbf{I}^A \delta^{AB}$ with either $\mathbf{I}^\tau \neq 0$ or $\mathbf{I}^\mu \neq 0$ (*e.g.* $\mathbf{I}^\tau \neq 0$ from RG running for not too large value of $\tan \beta$), or flavour violating correction $\mathbf{I}_{\text{th}}^{\mu\mu}$, or $\mathbf{I}_{\text{th}}^{e\tau}$.

There can be, of course, other interesting cases with more complicated interplay of RG and low energy threshold corrections [44, 46].

7. Summary

We have reviewed recent developments in exploring flavour dynamics in the supersymmetric extension of the Standard Model. Emphasis has been put on possible interesting effects in b -physics arising for large values of $\tan\beta$ and not too high a scale of the MSSM Higgs boson sector, both in the case of minimal flavour violation and in the case of flavour violation originating in the sfermion sector. We have discussed the importance of the flavour changing neutral Higgs boson couplings generated by the scalar penguin diagrams and their role in constraining the MSSM parameter space. We have shown that in the case of minimal flavour violation the experimental lower limit on $B_s^0-\bar{B}_s^0$ mass difference constrains branching fractions of the decays $B_{d,s}^0 \rightarrow \mu^+\mu^-$ possible in the MSSM. We have also pointed out that observation of the $B_d^0 \rightarrow \mu^+\mu^-$ decay with BR at the level $\gtrsim 3 \times 10^{-8}$ (and even lower if ΔM_s turns out to be bigger than 15/ps) would be a strong indication of nonminimal flavour violation in the quark sector. Flavour violation connected with neutrino oscillations has been also discussed. It has been argued that in some physically interesting situations flavour violation originating in the slepton mass matrices can be responsible (at least in part) for observed pattern of the neutrino mixing and mass squared differences.

We would like to thank A.J. Buras and Ł. Ślawniowska in collaboration with whom some of the results presented here have been worked out. The work was partly supported by the Polish State Committee for Scientific Research (KBN) grant 5 P03B 119 20 for 2001-2002 and by the EC Contract HPRN-CT-2000-00148 for years 2000-2004. The work of J.R. was also supported by the German Bundesministerium für Bildung und Forschung under the contract 05HT1WOA3 and the Deutsche Forschung Gemeinschaft Project Bu. 706/1-1.

REFERENCES

- [1] See *e.g.* A. Riotto, hep-ph/9807454.
- [2] M. Olechowski, S. Pokorski, *Phys. Lett.* **B214**, 393 (1988).
- [3] L. Wolfenstein, *Phys. Rev. Lett.* **51**, 1945 (1983).
- [4] A.J. Buras, M.E. Lautenbacher, G. Ostermaier, *Phys. Rev.* **D50**, 3433 (1994).
- [5] R. Aleksan, talk at the Planck 2002 Meeting, May 24–29, Kazimierz Dolny, Poland.
- [6] A.J. Buras, hep-ph/0101336.
- [7] A.J. Buras in *Probing the Standard Model of Particle Interactions*, eds. F. David, R. Gupta, Elsevier Science B.V., 1998.

- [8] C. Bernard *et al.*, *Nucl. Phys. Proc. Suppl.* **94**, 346 (2001); A. Ali Khan *et al.* (the CP-PACS Collaboration), *Phys. Rev.* **D64**, 034505 (2001).
- [9] C.R. Allton *et al.*, *Phys. Lett.* **B453**, 30 (1999).
- [10] D. Becirevic, V. Gimenez, G. Martinelli, M. Papinutto, J. Reyes, *J. High Energy Phys.* **0204**, 025 (2002); *Nucl. Phys. Proc. Suppl.* **106**, 385 (2002).
- [11] A.J. Buras, P.H. Chankowski, J. Rosiek, Ł. Ślawianowska, *Nucl. Phys.* **B619**, 434 (2001).
- [12] J. Rosiek hep-ph/0108226.
- [13] J. Flynn, C.T. Sachrajda in *Heavy Flavours II*, eds. A.J. Buras, M. Lindner, World Scientific Publishing Co., Singapore 1998.
- [14] A. Brignole, F. Feruglio, F. Zwirner, *Z. Phys.* **C71**, 679 (1996).
- [15] M. Misiak, S. Pokorski, J. Rosiek in *Heavy Flavours II*, eds. A.J. Buras, M. Lindner, World Scientific Publishing Co., Singapore 1998; *Adv. Ser. Direct. High Energy Phys.* **15**, 795 (1998).
- [16] Hamzaoui, M. Pospelov, M. Toharia, *Phys. Rev.* **D59**, 095005 (1999).
- [17] K. Babu, C. Kolda, *Phys. Rev. Lett.* **84**, 228 (2000).
- [18] P.H. Chankowski, S. Pokorski in *Perspectives on Supersymmetry*, G.L. Kane ed., World Scientific 1998.
- [19] P.H. Chankowski, Ł. Ślawianowska, *Phys. Rev.* **D63**, 054012 (2001); *Acta Phys. Pol.* **B32**, 1895 (2001).
- [20] A.J. Buras, P.H. Chankowski, J. Rosiek, Ł. Ślawianowska, in preparation.
- [21] J. Rosiek, *Phys. Rev.* **D41**, 3464 (1990); hep-ph/9511250.
- [22] A.J. Buras, S. Jäger, J. Urban, *Nucl. Phys.* **B605**, 600 (2001).
- [23] G. Isidori, A. Retico, *J. High Energy Phys.* **0111**, 001 (2001).
- [24] G. Degrassi, P. Gambino, G.-F. Giudice, *J. High Energy Phys.* **0012**, 009 (2000).
- [25] M. Carena, D. Garcia, U. Nierste, C.E.M. Wagner, *Phys. Lett.* **B499**, 141 (2001).
- [26] C. Bobeth, T. Ewerth, F. Krüger, J. Urban, *Phys. Rev.* **D64**, 074014 (2001).
- [27] G. Buchalla, A.J. Buras, *Nucl. Phys.* **B400**, 225 (1993).
- [28] P. Ball, R. Fleischer, G.F. Tartarelli, P. Vikas, G. Wilkinson (conveners), hep-ph/0003238.
- [29] F. Gabbiani, E. Gabrielli, A. Masiero, L. Silvestrini, *Nucl. Phys.* **B477**, 321 (1996).
- [30] M. Ciuchini *et al.*, *J. High Energy Phys.* **9810**, 008 (1998).
- [31] S. Bertolini, F.M. Borzumati, A. Masiero, G. Ridolfi, *Nucl. Phys.* **B353**, 591 (1991); N. Oshimo, *Nucl. Phys.* **B404**, 20 (1993); C.-S. Huang, Q.-S. Yan, *Phys. Lett.* **B442**, 3811 (1998); C.-S. Huang, W. Liao, Q.-S. Yan, *Phys. Rev.* **D59**, 011701 (1999); S.R. Chaudhury, N. Gaur, *Phys. Lett.* **B451**, 86 (1999); C.-S. Huang, W. Liao, Q.-S. Yan, S.-H. Zhu, *Phys. Rev.* **D63**, 114021 (2001); *Phys. Rev.* **D64**, 059902 (2001).
- [32] G. Isidori, hep-ph/0101121.

- [33] A. Masiero, H. Murayama, *Phys. Rev. Lett.* **83**, 907 (1999).
- [34] D. Becirevic *et al.*, hep-ph/0112303.
- [35] Z. Maki, M. Nakagawa, S. Sakata, *Prog. Theor. Phys.* **28**, 870 (1962).
- [36] Y. Fukuda *et al.*, [The SuperKamiokande Collaboration], *Phys. Rev. Lett.* **81**, 1562 (1998); S. Fukuda *et al.* (The SuperKamiokande Collaboration), *Phys. Rev. Lett.* **85**, 3999 (2000).
- [37] Q.R. Ahmad *et al.* (The SNO Collaboration), *Phys. Rev. Lett.* **87**, 071301 (2001).
- [38] K. Nishikawa, plenary talk at the *Int. EPS Conference on High Energy Physics*, July 2001, Budapest, Hungary.
- [39] M. Apollonio *et al.* (The CHOOZ Collaboration), *Phys. Lett.* **B466**, 415 (1999).
- [40] S. Lavignac, I. Masina, C.A. Savoy, *Phys. Lett.* **B520**, 269 (2001); *Nucl. Phys.* **B633**, 139 (2002).
- [41] P.H. Chankowski, Z. Płuciennik, *Phys. Lett.* **B316**, 312 (1993); K.S. Babu, C.N. Leung, J. Pantaleone, *Phys. Lett.* **B319**, 191 (1993); S. Antusch, M. Drees, J. Kersten, M. Lindner, M. Ratz, *Phys. Lett.* **B519**, 238 (2001).
- [42] P.H. Chankowski, W. Królikowski, S. Pokorski, *Phys. Lett.* **B473**, 109 (2000); J.A. Casas, J.R. Espinosa, A. Ibarra, I. Navarro, *Nucl. Phys.* **B573**, 652 (2000).
- [43] E.J. Chun, S. Pokorski, *Phys. Rev.* **D62**, 053001 (2002).
- [44] E.J. Chun, *Phys. Lett.* **B505**, 155 (2001).
- [45] P.H. Chankowski, P. Wąsowicz, *Eur. Phys. J.* **C23**, 249 (2002).
- [46] P.H. Chankowski, S. Pokorski, *Int. J. of Mod. Phys.* **A17**, 575 (2002).